Rare Earth Element β-Diketone Complexes as Novel Corrosion Inhibitors for 304 and 316 Stainless Steel in 0.1 M HCl Solution

Olatunde .J. Lawal & Johannes .H. Potgieter

University of the Witwatersrand

ABSTRACT

The corrosion inhibition of austenitic stainless steel (304 and 316 SS) in 0.1M HCl solution was investigated in the temperature range of 20–60°C, using cerium and lanthanum acetylacetone and hexafluoroacetylacetone as potential green and novel corrosion inhibitors. Weight loss and potentiodynamic polarisation methods as well as surface analyses were used to investigate the effectiveness of these inhibitors in 0.1 M HCl solution. Experimental results showed that the rare earth element REE β-diketone complexes are effective inhibitors to reduce the corrosion of 304 and 316 SS. Polarisation measurements indicated that the $Ce(acac)_3$, $La(acac)_3$, $Ce(hfac)_3$ and $La(hfac)_3$ acted as cathodic inhibitors. The nature of the metal surface after exposure to the corrosive solution, was analysed by SEM and FTIR spectra, as well as Raman spectroscopy. Scanning electron microscopy (SEM) and Raman spectroscopy confirmed the formation of protective films of the inhibitors on the steel surfaces. The effect of temperature on the corrosion rate and inhibition efficiencies were also determined, and it was found that as the temperature increased, there was an increase in corrosion rate and decrease in inhibition efficiency.

Keywords: stainless steels; corrosion inhibitors; REE β-diketone; polarisation; raman spectroscopy.

Classification: DDC Code: 150.195 LCC Code: BF408

Language: English

London Journals Press

LJP Copyright ID: 925685
Print ISSN: 2631-8490
Online ISSN: 2631-8504

London Journal of Research in Science: Natural and Formal

Volume 22 | Issue 8 | Compilation 1.0

Rare Earth Element β-Diketone Complexes as Novel Corrosion Inhibitors for 304 and 316 Stainless Steel in 0.1 M HCl Solution

Olatunde .J. Lawal[α] & Johannes .H. Potgieter[σ]

ABSTRACT

The corrosion inhibition of austenitic stainless steel (304 and 316 SS) in 0.1M HCl solution was investigated in the temperature range of 20–60°C, using cerium and lanthanum acetylacetone and hexafluoroacetylacetone as potential green and novel corrosion inhibitors. Weight loss and potentiodynamic polarisation methods as well as surface analyses were used to investigate the effectiveness of these inhibitors in 0.1 M HCl solution. Experimental results showed that the rare earth element REE β-diketone complexes are effective inhibitors to reduce the corrosion of 304 and 316 SS. Polarisation measurements indicated that the $Ce(acac)_3$, $La(acac)_3$, $Ce(hfac)_3$ *and* $La(hfac)_3$ *acted as cathodic inhibitors. The nature of the metal surface after exposure to the corrosive solution, was analysed by SEM and FTIR spectra, as well as Raman spectroscopy. Scanning electron microscopy (SEM) and Raman spectroscopy confirmed the formation of protective films of the inhibitors on the steel surfaces. The effect of temperature on the corrosion rate and inhibition efficiencies were also determined, and it was found that as the temperature increased, there was an increase in corrosion rate and decrease in inhibition efficiency.*

Keywords: stainless steels; corrosion inhibitors; REE β-diketone; polarisation; raman spectroscopy.

Author α: School of Chemical and Metallurgical Engineering, University of the Witwatersrand, Private Bag X3, Wits, 2050, South Africa.
σ: Department of Natural Science, Faculty of Science and Engineering, Manchester Metropolitan University, Manchester, M1 5GD, UK.

I. INTRODUCTION

Metallo-organic compounds of β-diketone are widely used due to their diverse application in the field of coordination chemistry research [1–3]. Among these compounds are rare earth element (REE) β-diketone complexes with a general formula of $M(RCOCHCOR')_n$ (where M is a rare earth metal, and R and R' represent alkyl, aryl, chlorinated alkyl, chlorinated aryl or phenyl group) which are produced from a reaction between a rare earth halide and various dicarbonyl compounds (β-diketone). Most investigations reported in the literature on REEs compounds as corrosion inhibitors have been related to the application of REE oxides, chlorides, sulphates and nitrates. They have been reported to be suitable and effective corrosion inhibitors for various steels, aluminium and other alloys in various corrosive environments [4–9].

Austenitic stainless steels (304 and 316) are some of the most widely used metals in a range of industries due to their good mechanical strength and excellent resistance to corrosion [10–13]. However, they are still susceptible to corrosion in an environment that is highly aggressive which contains chloride ions [14,15]. To mitigate the effect of the chloride ions, a corrosion inhibitor is frequently added to the environment to prevent localised forms of corrosion on the surface of the steel.

Ghanbari et al. [16] investigated the inhibitive potential of acetylacetone complexes of transition metals (zinc(II), manganese(II), cobalt(II), and copper(II)) at concentrations of 0.01 M at 25°C in 1M phosphoric acid (H_3PO_4), the same H_3PO_4 solution was added separately with another

solution of 0.1 M HCl, and also with 0.1 M NaCl, so that both NaCl and HCl solution would provide chloride ions in the solution. They reported that the addition of acetylacetone complexes to H_3PO_4 and to the two separate acidic chloride solutions shifted the corrosion potential of the mild steel toward more negative potentials. At the same time, there was an increase in the cathodic Tafel slopes, suggesting that the acetylacetone complexes acted as cathodic inhibitors. In solutions of NaCl with H_3PO_4 and HCl with H_3PO_4, the inhibition efficiency of the acetylacetonate complexes increased, giving a corresponding reduction in the corrosion rates.

Somers et al. [17] studied the effect of rare-earth (La, Ce, Nd, and Y) 3-(4-methyl benzoyl) propanoate compounds (REE$(mbp)_3$) with additions at a concentration of 0.25 mM on the corrosion behaviour of mild steel in 0.01 M NaCl. Detailed surface analysis after immersion revealed that the inhibitors significantly improved the corrosion resistance of mild steel in the NaCl solution. FTIR and EDS showed the presence of a thin film containing inhibitor components on the surface of the tested steel specimens.

Markley et al. [18] tested the inhibition effectiveness of cerium diphenyl phosphate ($Ce(dpp)_3$) for corrosion inhibition of an aluminium alloy (AA2024-T3) in 0.1 M NaCl solution at 25 C. A concentration of 200 ppm $Ce(dpp)_3$ resulted in a high level of corrosion protection with no evidence of corrosion product or pitting.

No previous reports could be found in the literature describing the application of REE β-diketones as potential corrosion inhibitors for the corrosion prevention of stainless steels in acidic media. In this paper, cerium and lanthanum acetylacetone, as well as hexafluoroacetylacetone, will be the focal point as a possible replacement for hexavalent chromium-based corrosion inhibitors for 304 and 316 stainless steels in 0.1 M HCl solution. The investigation will endeavour to establish whether these inhibitors are effective, and also whether they act as anodic, cathodic, or mixed inhibitors.

II. EXPERIMENTAL SECTION

2.1 Materials and Preparation

The 304 SS had the following composition (wt. %): C, 0.05; Mn, 0.15; Si, 0.320; S, 0.019; Cr, 18.5, Mo, 0.46; Ni, 9.0; Fe, balance and while the 316 SS contained (wt. %): C, 0.05; Mn, 0.10; Si, 0.57; S, 0.007; Cr, 17.0, Mo, 2.0; Ni, 11.0; Fe, balance. The samples were all cut to dimensions of 2 cm × 3 cm × 0.12 cm and a 3.0 mm diameter hole was drilled at the edge for suspending the samples into solution. The samples were ground sequentially with silicon carbide papers, starting with 500 grit followed by 800, 1000, 1200, 2400, and 2800 grit until a mirror-like surface was achieved. The prepared samples were rinsed with distilled water, followed by ethanol, and air-dry. For electrochemical measurements, the same materials that were used for the weight loss experiment were mechanically cut to a dimension of 1.0 cm × 0.7 cm × 0.12 cm. These samples were then mounted using a resin with a conductible cable attached to the samples and successively abraded using the same series of silicon carbide papers as before. The exposed surface area of the samples was 0.7 cm², while the rest of the sample was encased by resin. Before the experiments, specimens were washed with distilled water, degreased in ethanol, and dried.

Analytical grade 32 % concentrated HCl obtained from Merck (Pty) Ltd was diluted with distilled water to prepare the 0.1 M HCl solutions. The cerium and lanthanum acetylacetone and hexafluoroacetylacetone were synthesised in accordance with the method described in the literature [19–21]. The chemical reaction is as follows:

$$MX_n.y\left(H_2O\right) + nRCOCH_2COR'\ METHANOL \rightarrow M(RCOCHCOR')_n.yH_2O + nHX \ldots \quad 1$$

where M is the rare earth metal. The structural formulae of the REE β-diketones compounds are shown in Figure 1.

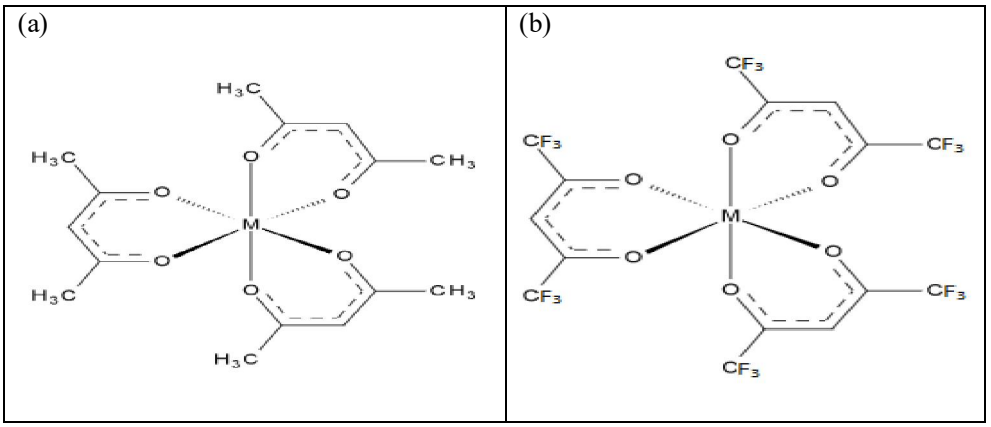

Figure 1: Chemical structures of (a) metal acetylacetonate and (b) metal hexafluoroacetylacetone, where M = Ce or La, Modified from [22].

2.2 Surface Aanalysis

A Zeiss (51-ADD0048) Scanning Electron Microscope (SEM) instrument operating at 15kV coupled with energy-dispersive X-ray spectroscopy (EDS) was used to study the surface morphology of the 304 and 316 SS after immersion in media with and without inhibitor. The characterisation of the REE complexes and the mapping of the surface of the steels were further carried out using Raman Spectroscopy and Fourier Transform Attenuated Total Reflectance Infrared Spectroscopy (FT-ATR-IR). Using a Perkin Elmer Spectrum-2 instrument, the FT-IR spectra were recorded in a frequency range of 420–4000 cm^{-1}. The Raman spectra were acquired using the 514.5 nm line of a Lexel Model 95 SHG argon-ion laser as an excitation source and a Horiba LabRAM HR Raman spectrometer equipped with a high-sensitivity Olympus BX41 microscope. The data were acquired using LabSpec v5 software, and the spectra were obtained in the range of 3500-50 cm^{-1}.

2.3 Weight Loss Measurements

The weight loss measurements were performed at room temperature after immersion in 250 mL 0.1 M HCl solution without and with 0.5% wt. (m/v) inhibitor for 7 days. Triplicate experiments were conducted for each and the average weight losses with standard deviation were determined. The average weight losses were then used to calculate the corrosion rates (in µm/y) and inhibition efficiencies according to the following equations:

$$Corrosion\ rate\ (CR) = 3.65\ x\ 10^{6}\frac{W_0 - W_1}{DAT} \qquad (2)$$

Where W_0 and W_1 are the mass of the coupon (in grams) before and after immersion, respectively; D is the density of the coupon (in g/cm^3); T is the time of exposure (in days) and A is the exposed area of the coupon in the test solution (in cm^2).

$$Corrosion\ rate\ (CR) = 3.65\ x\ 10^{6}\frac{W_0 - W_1}{DAT} \qquad (3)$$

where CR and CR_i are the average corrosion rates of the uninhibited and inhibited steel samples, respectively.

2.4 Potentiodynamic Polarisation Experiments

Potentiodynamic polarisation studies were carried out using a Metrohm Autolab-1 Potentiostat/ Galvanostat equipped with Nova 2.1 software. A three-electrode setup was employed using a graphite counter electrode and Ag/AgCl (3 M KCl) as a reference electrode (all potentials are quoted with respect to this reference electrode). The stainless steel samples were the working electrodes in the system with an exposed surface of 0.7 cm^2 were immersed in the HCl solutions with and without inhibitor and the open circuit potential was measured after 30 min. Potentiodynamic polarisation studies were performed with a scan rate of 5 mV/s in the potential range from 200 mV below the corrosion potential to 800 mV above the corrosion

potential. Measurements were done at 20, 40, and 60˚C. The corrosion parameters, such as corrosion potential (E_{corr}), Tafel slopes (βa and βc), corrosion current density (i_{corr}) and corrosion rate were obtained from the current density-potential graphs using the Nova 2.1 software.

III. RESULTS AND DISCUSSION

3.1 Weight Loss Measurement

The inhibition of the corrosion of 304 SS and 316 SS after exposure to solutions without and with 0.5% wt. (m/v) concentrations of $Ce(acac)_3$, $La(acac)_3$, $Ce(hfac)_3$ and $La(hfac)_3$ inhibitors were examined at room temperature (approximately 25°C) using weight loss measurements. After seven days of immersion in each solution, the average corrosion rate was calculated and the results are presented in Table 1. At 0.5% wt. (m/v) concentration of $Ce(acac)_3$, $La(acac)_3$, $Ce(hfac)_3$ and $La(hfac)_3$ were 100% effective as no weight loss was observed. The excellent inhibition performance could be as a result of the adsorption of a passive film of REE β-diketone complexes on the steel surface. These results are in line with the report by Desa & Desai [23], where they used dicarbonyl compounds as a corrosion inhibitor for mild steel at room temperature and in a concentration range of 0.39-0.42 mol/L in 6 N HCl solution for 24 hours.

Table 1: Comparison of corrosion rates of 304 SS and 316 SS and the inhibition efficiency in the absence and presence of $Ce(acac)_3$, $La(acac)_3$, $Ce(hfac)_3$ and $La(hfac)_3$ in 0.1 M HCl solution.

	REE β-diketone	CR_i with inhibitor (μm/y)	SD	CR without inhibitor (μm/y)	IE (%)	Standard Deviation
304 SS	$Ce(acac)_3$	0.0	0.0	1.0	100	0.5
	$La(acac)_3$	0.0	0.0	0.8	100	0.3
	$Ce(hfac)_3$	0.0	0.0	0.7	100	0.3
	$La(hfac)_3$	0.0	0.0	0.8	100	0.3
316 SS	$Ce(acac)_3$	0.0	0.0	0.8	100	0.3
	$La(acac)_3$	0.0	0.0	0.8	100	0.3
	$Ce(hfac)_3$	0.0	0.0	0.8	100	0.3
	$La(hfac)_3$	0.0	0.0	0.3	100	0.6

3.2 Potentiodynamic Polarisation Measurements

Polarisation curves of 304 and 316 SS at 20, 40, and 60°C measure in HCl solutions without inhibitor and with $Ce(acac)_3$, $La(acac)_3$, $Ce(hfac)_3$ and $La(hfac)_3$ inhibitors are shown in Figures 2 and 3. The electrochemical parameters derived from these curves are summarised in Tables 2 and 3. The E_{corr} in solutions containing each of the inhibitors shifted towards more negative potentials (less noble) compared to E_{corr} when there was no inhibitor present in the solution. The downward decrease in the value of E_{corr} indicated that all of the inhibitors act as cathodic inhibitors [9]. As expected, the corrosion rates and current densities increased with increasing temperature. It is noteworthy that the inhibition efficiencies of the REE β-diketones obtained were very similar to the inhibition efficiencies obtained by Ghanbari et al. [16] when they used acetylacetone complexes of transition metals for corrosion inhibition of mild steel in a 1 M phosphoric acid solution. A similar observation was observed when Desa & Desai [23] used different carbonyl compounds as a corrosion inhibitor for mild steel at a fixed concentration of

inhibitors while varying the concentration of the HCl solution from 1.0, 2.0, 3.0 and 4.0 N. Potentiodynamic polarisation studied of these compounds showed that the inhibition efficiencies of all the tested compounds increase from 22 up to 98% depends on the concentration of the HCl solution that was used. The corrosion rates were found to be increased as the concentration of HCl solution increases from 1.0, 2.0, 3.0 and 4.0 N.

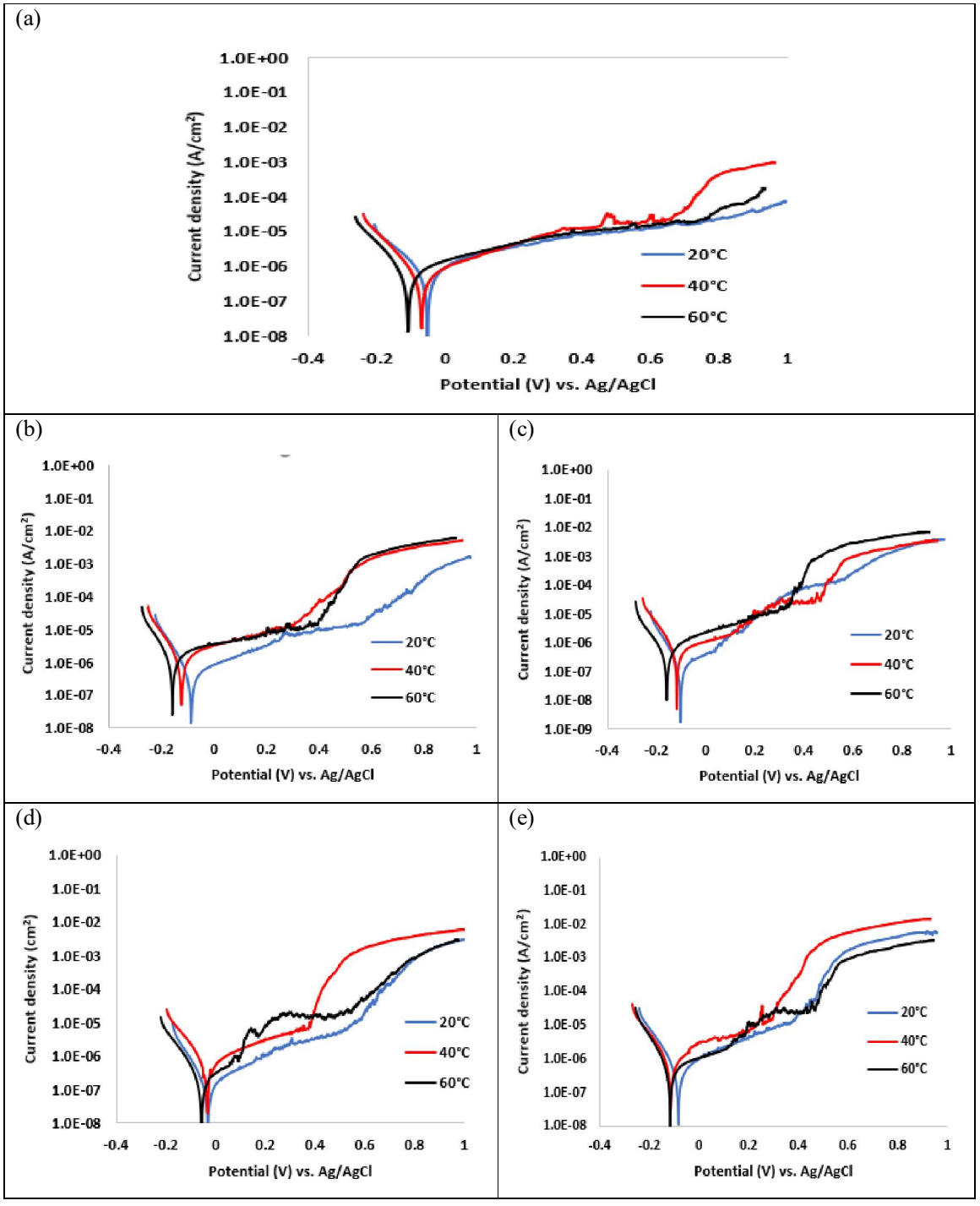

Figure 2: Potentiodynamic polarisation curves of 304 SS in 0.1 M HCl solution (a) without inhibitor and with (b) $Ce(acac)_3$, (c) $La(acac)_3$, (d) $Ce(hfac)_3$ and (e) $La(hfac)_3$ inhibitors.

Table 2: Electrochemical parameters of 304 SS obtained from potentiodynamic polarisation curves measured in 0.1 M HCl solution and with corrosion inhibitors $Ce(acac)_3$, $La(acac)_3$, $Ce(hfac)_3$ and $La(hfac)_3$ present in the solution. The results presented in Table 2 were derived from Figure 2.

0.1 M HCl solution without inhibitor						
Temp. (°C)	E_{corr} (V)	i_{corr} (A/cm²)	βa (mV/dec)	βc (mV/dec)	CR (µm/y)	IE (%)
20	-0.051	4.82×10^{-7}	44	133	4.99	
40	-0.068	4.93×10^{-7}	42	120	5.11	
60	-0.108	5.05×10^{-7}	45	125	5.23	
$Ce(acac)_3$						
Temp. (°C)	E_{corr} (V)	i_{corr} (A/cm²)	βa (mV/dec)	βc (mV/dec)	CR (µm/y)	IE (%)
20	-0.082	2.74×10^{-7}	26	87	2.84	43
40	-0.136	2.92×10^{-7}	52	87	3.02	41
60	-0.157	3.07×10^{-7}	45	104	3.18	39
$La(acac)_3$						
Temp. (°C)	E_{corr} (V)	i_{corr} (A/cm²)	βa (mV/dec)	βc (mV/dec)	CR (µm/y)	IE (%)
20	-0.128	2.79×10^{-7}	22	85	2.89	42
40	-0.109	2.95×10^{-7}	25	87	3.06	40
60	-0.160	3.17×10^{-7}	35	96	3.28	37
$Ce(hfac)_3$						
Temp. (°C)	E_{corr} (V)	i_{corr} (A/cm²)	βa (mV/dec)	βc (mV/dec)	CR (µm/y)	IE (%)
20	-0.030	2.69×10^{-7}	28	92	2.79	44
40	-0.036	2.93×10^{-7}	19	102	3.03	40
60	-0.059	3.16×10^{-7}	42	122	3.27	37
$La(hfac)_3$						
Temp. (°C)	E_{corr} (V)	i_{corr} (A/cm²)	βa (mV/dec)	βc (mV/dec)	CR (µm/y)	IE (%)
20	-0.083	2.61×10^{-7}	36	90	2.73	45
40	-0.094	2.88×10^{-7}	12	97	3.00	42
60	-0.115	3.13×10^{-7}	43	97	3.26	38

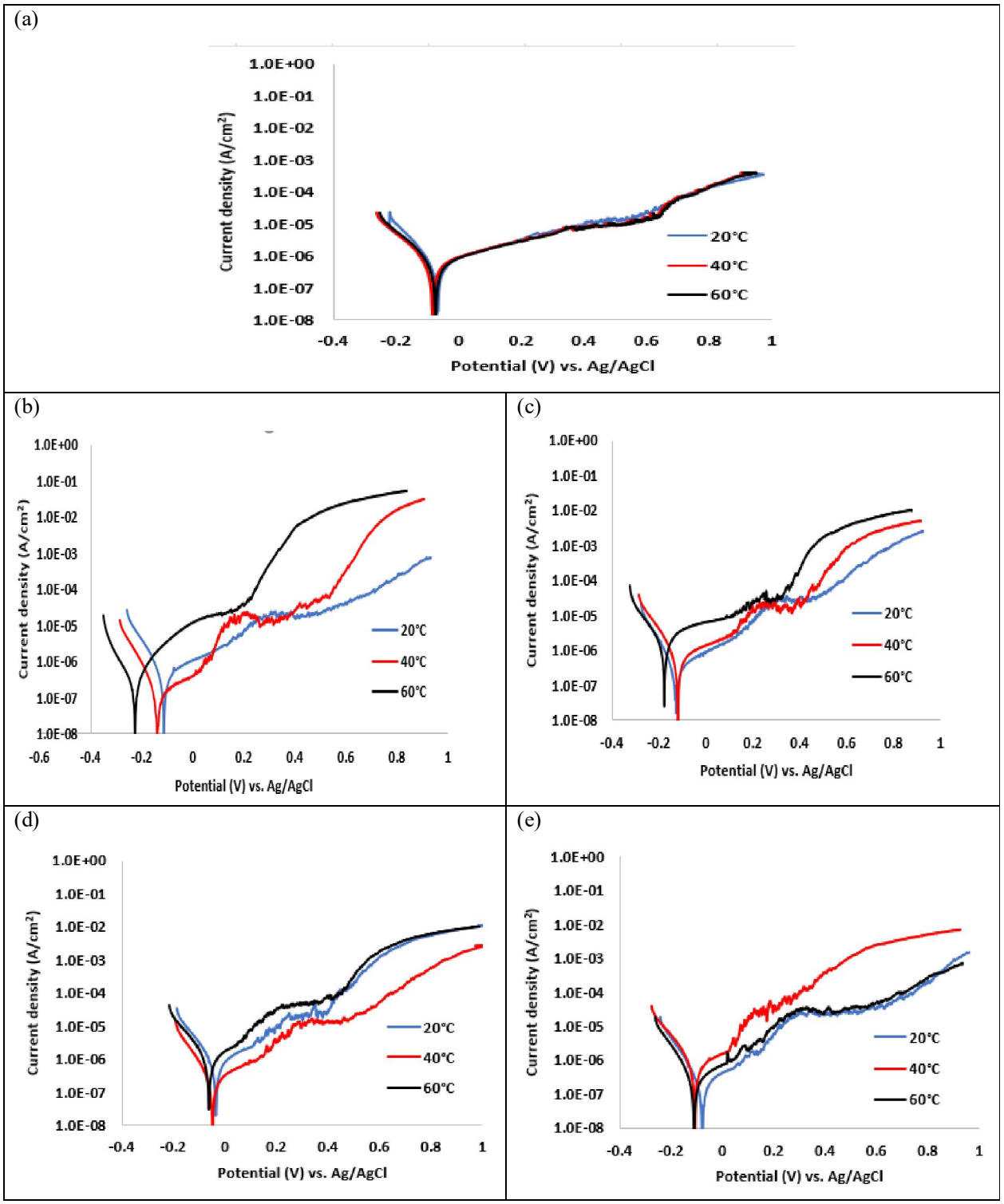

Figure 3: Potentiodynamic polarisation curves of 316 SS in 0.1 M HCl solution (a) without inhibitors and with (b) $Ce(acac)_3$, (c) $La(acac)_3$, (d) $Ce(hfac)_3$ and (e) $La(hfac)_3$ inhibitors.

Table 3: Electrochemical parameters of 316 SS obtained from potentiodynamic polarisation curves measured in 0.1 M HCl solution and with corrosion inhibitors $Ce(acac)_3$, $La(acac)_3$, $Ce(hfac)_3$ and $La(hfac)_3$ present in the solution. The results presented in Table 3 were derived from Figure 3.

0.1 M HCl solution without inhibitor						
Temp. (°C)	E_{corr} (V)	i_{corr} (A/cm²)	βa (mV/dec)	βc (mV/dec)	CR (µm/y)	IE (%)
20	-0.067	3.25×10^{-7}	39	110	3.39	
40	-0.081	3.60×10^{-7}	42	122	3.76	
60	-0.109	4.24×10^{-7}	42	15	4.43	
$Ce(acac)_3$						
Temp. (°C)	E_{corr} (V)	i_{corr} (A/cm²)	βa (mV/dec)	βc (mV/dec)	CR (µm/y)	IE (%)
20	-0.108	1.70×10^{-7}	38	102	1.78	48
40	-0.126	1.92×10^{-7}	37	106	2.00	47
60	-0.205	2.28×10^{-7}	57	109	2.38	46
$La(acac)_3$						
Temp. (°C)	E_{corr} (V)	i_{corr} (A/cm²)	βa (mV/dec)	βc (mV/dec)	CR (µm/y)	IE (%)
20	-0.137	1.79×10^{-7}	36	99	1.87	45
40	-0.119	2.00×10^{-7}	39	99	2.09	44
60	-0.177	2.27×10^{-7}	43	105	2.37	42
$Ce(hfac)_3$						
Temp. (°C)	E_{corr} (V)	i_{corr} (A/cm²)	βa (mV/dec)	βc (mV/dec)	CR (µm/y)	IE (%)
20	-0.108	1.68×10^{-7}	38	102	1.76	48
40	-0.126	1.91×10^{-7}	37	106	2.00	47
60	-0.205	2.35×10^{-7}	57	109	2.46	45
$La(hfac)_3$						
Temp. (°C)	E_{corr} (V)	i_{corr} (A/cm²)	βa (mV/dec)	βc (mV/dec)	CR (µm/y)	IE (%)
20	-0.076	1.73×10^{-7}	30	92	1.81	47
40	-0.086	1.93×10^{-7}	26	84	2.12	46
60	-0.105	2.32×10^{-7}	31	115	2.33	45

IV. SURFACE ANALYSES

4.1 Scanning Electron Microscopy (Sem)

The surface morphology of the 304 and 316 SS samples with and without inhibitor after potentiodynamic polarisation tests in 0.1 M HCl solution as determined by SEM are shown in Figures 4 and 5. The micrographs of both samples in the absence of an inhibitor showed damage to the surface, with a deep and wide hole on a 304 SS suggesting an attack by chloride ions. In the presence of the inhibitors, EDS results (Figures 6 and 7) indicate the film formation on the metal surface, which could be responsible for corrosion inhibition. It is noteworthy that the tested inhibitors provide a uniform film coverage on the surface of the steel at all temperatures and at a low concentration (0.5% m/v), with no evidence of localised corrosion occurring. EDS analysis was carried out to identify the constituents of the film on the steel surface and the results revealed that

the film primarily consists of a rare earth element (Ce or La), oxygen (O), and other elements (Fe, Cr, Ni) that were major constituents of the steel, as indicated in Figures 6 and 7. These results were consistent with the investigation carried out by Peng et al. [24] when they studied rare-earth 3- (4-methylbenzoyl) - propanoate compounds ($Ce(dpm)_3$ and $La(dpm)_3$) as corrosion inhibitors for mild steel in 0.1 M NaCl solutions. SEM/EDS analyses showed the steel surface was protected by $Ce(dpm)_3$ and $La(dpm)_3$ despite being used at a low concentration of 0.25 mM. EDS also indicated that a dense layer of deposit on the surface of the steel contained rare earth elements (Ce and La) and iron (Fe). This is presumably due to the deposit consisting of a mixture of a rare-earth rich film (rare earth oxide or hydroxide) as well as iron oxide/ hydroxide.

Nam et al. [25] investigated the corrosion behaviour of copper alloy using 0.15 mM concentration of yttrium 3-(4-nitrophenyl)-2-propenoate ($Y(4NO_2Cin)_3$ inhibitor and 0.1 M NaCl solution as a corrosive medium. SEM analysis was conducted on the copper alloy that was immersed in a chloride solution with and without ($Y(4NO_2Cin)_3$ for a period of 20 hours. Micrographs obtained from SEM revealed that $Y(4NO_2Cin)_3$ actively impedes corrosion of copper alloy with no corrosion attack occurring on the copper surface after immersion for 20 hours. When the same experiment was repeated in the absence of $Y(4NO_2Cin)_3$ under the same conditions, deep penetration of chloride ions with a great level of corrosion was observed, suggesting that $Y(4NO_2Cin)_3$ inhibits the corrosion of copper alloy in 0.1 M sodium chloride solution.

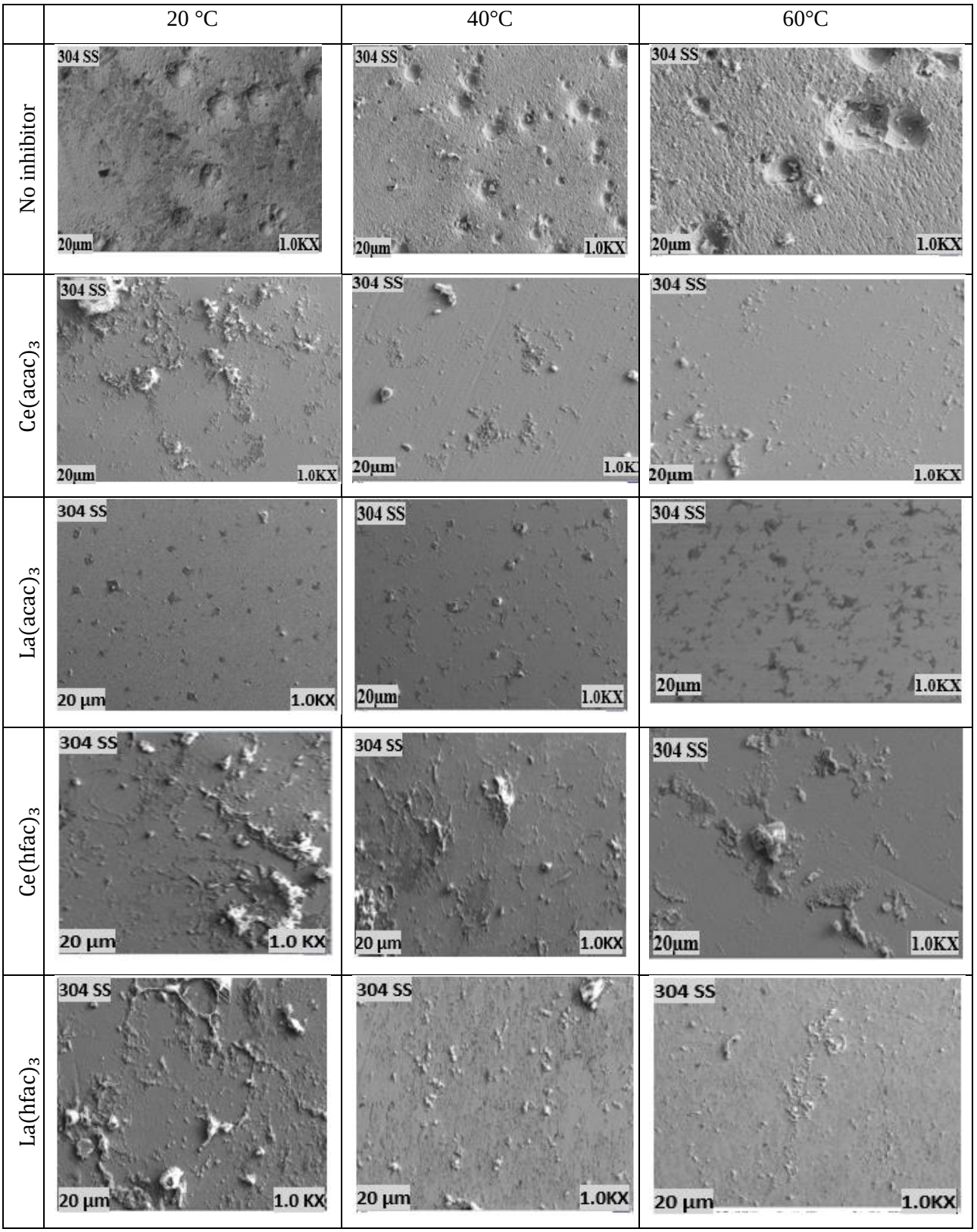

Figure 4: SEM micrographs of 304 SS sample surfacesin the absence and presence of $Ce(acac)_3$ and $La(acac)_3$ after exposure to 0.1 M HCl solutions at 20, 40 and 60°C.

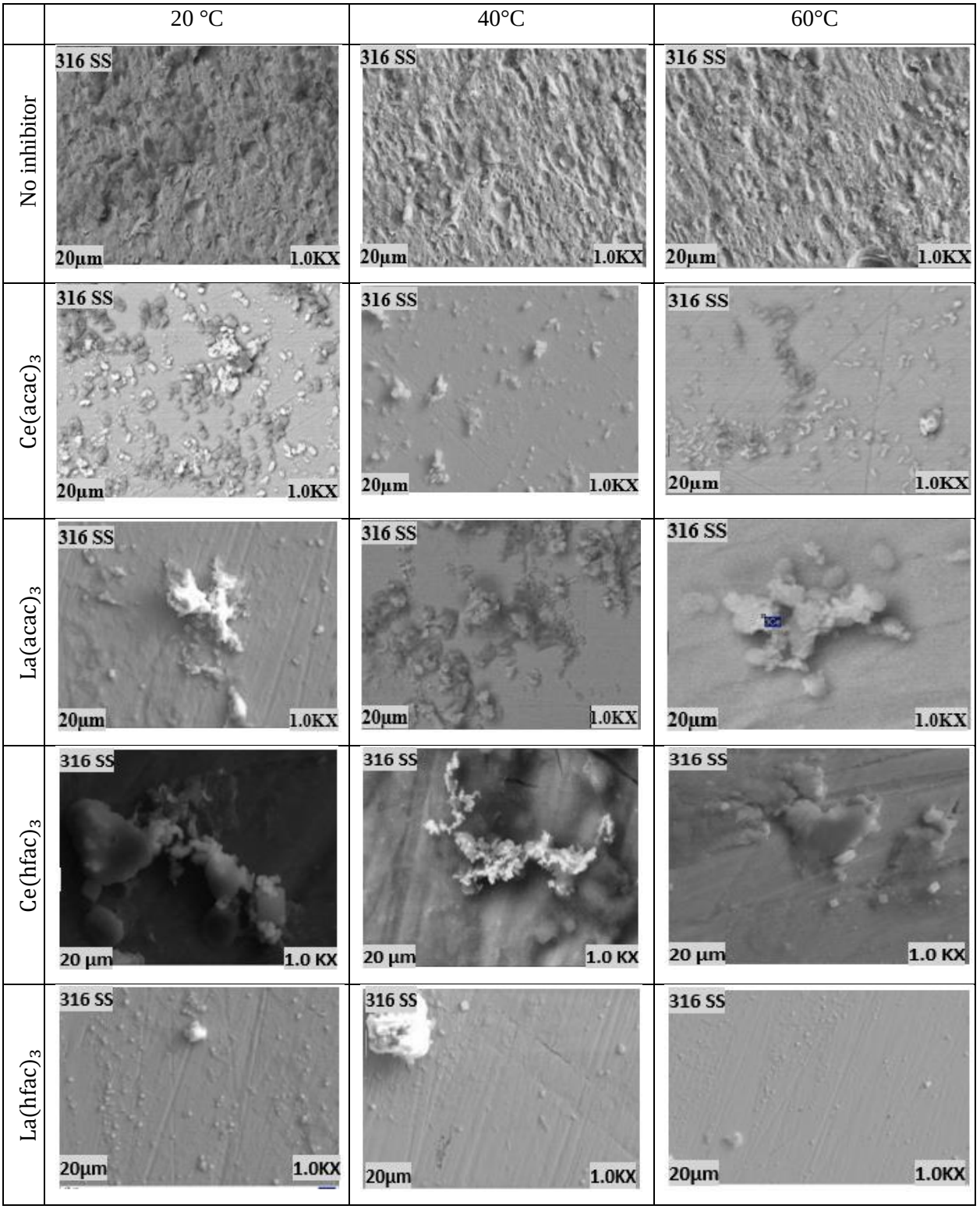

Figure 5: SEM micrographs of 316 SS sample surfaces in the absence and presence of $Ce(acac)_3$, $La(acac)_3$, $Ce(hfac)_3$ and $La(hfac)_3$ after exposure to 0.1 M HCl solutions at 20, 40 and 60°C.

(a)

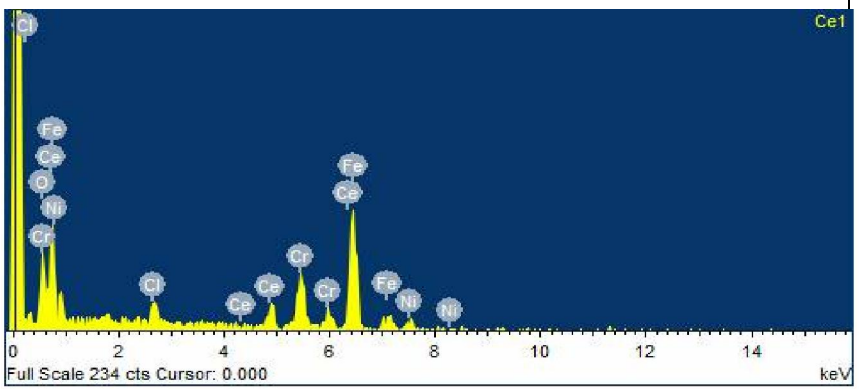

Element	Weight %	Atomic %
O K	9.20	27.20
Cl K	2.41	3.22
Cr K	15.99	14.55
Fe K	54.43	46.12
Ni K	6.07	4.89
Ce L	11.90	4.02
Totals	100.00	

(b)

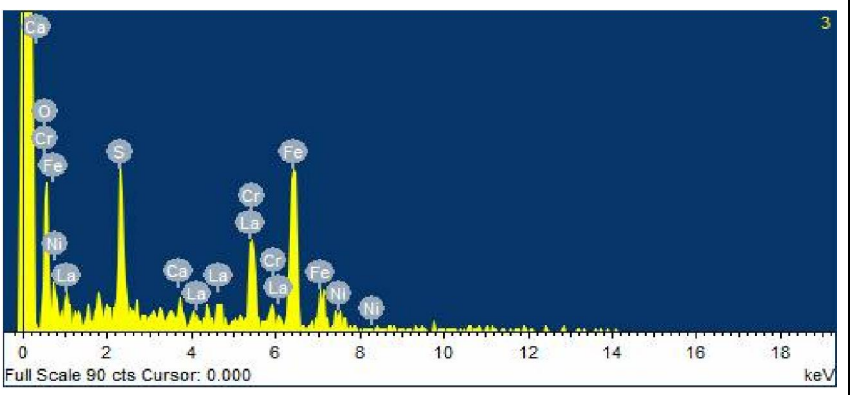

Element	Weight %	Atomic %
O K	14.32	36.20
Cr K	15.03	11.69
Fe K	48.56	35.15
Ni K	5.90	4.07
La L	16.19	12.89
Totals	100.00	

Figure 6: EDS of 304 SS after exposure to a HCl solution containing (a) $Ce(acac)_3$ at 20°C and (b) $La(acac)_3$ at 60°C with inhibitors at 0.5 % wt. (m/v) concentration.

(c)

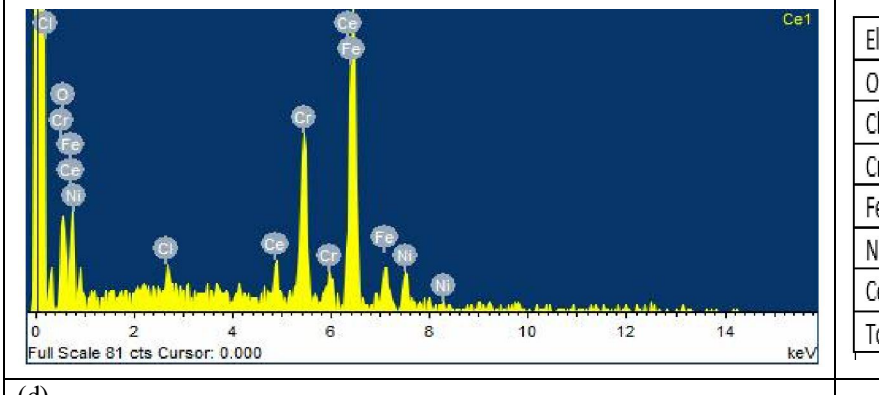

Element	Weight %	Atomic %
O K	3.82	12.56
Cl K	0.62	0.91
Cr K	18.64	18.83
Fe K	59.00	55.48
Ni K	10.59	9.48
Ce L	7.32	2.74
Totals	100.00	

(d)

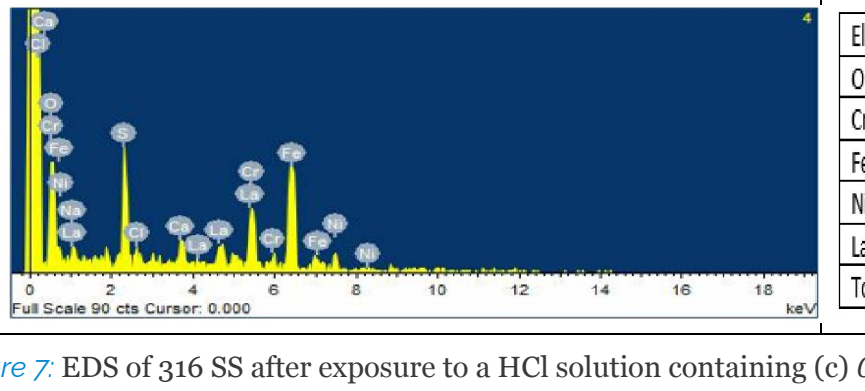

Element	Weight %	Atomic %
O K	11.41	29.46
Cr K	12.98	10.31
Fe K	44.63	33.00
Ni K	6.61	4.65
La L	24.37	22.58
Totals	100.00	

Figure 7: EDS of 316 SS after exposure to a HCl solution containing (c) $Ce(hfac)_3$ 20°C and (d) $La(hfac)_3$ at 60°C with inhibitors at 0.5 % wt. (m/v) concentration.

4.2 Raman Spectroscopy

Raman Spectroscopy was employed to map the surface of the steel samples after performing electrochemical tests in a corrosive medium that contained the REE β-diketones in order to further investigate the nature of the corrosion inhibitors' action. The Raman spectra for the synthesised REE β-diketone powders and the film layer deposited on the steel surface after the electrochemical tests are shown in Figure 8. The frequency shifts identified in the Raman spectra were compared with published results and they confirmed the formation of the REE β-diketone complexes [26] and complex film formation on the surface of the steel [27]. For the steel surface exposed to REE β-diketone complex inhibited solution, the bands associated with carbonyl functional group (C=O) and enolic group (OH) disappear. The disappearance of these bands may be attributed to the coordination between the steel, the enolic structure and the carbonyl function group resulting in the formation of a protective layer of rare earth oxide or hydroxide $REE(OH)_3$ [18]. The Raman shift with frequency bands at ~248 and ~1311 cm^{-1}, and at 377 cm^{-1} could be assigned to stretching vibrations which correspond to hematite (α-Fe_2O_3) and lepidocrocite (γ-FeOOH), respectively [7,28–30]. Details of the frequency bands with the associated functional groups for the spectra peaks are shown in Table 4. Raman analysis for the corrosion product tests was done on samples 304 SS doped in solutions containing $Ce(acac)_3$ or $La(acac)_3$ and 316 SS doped in solutions containing $Ce(hfac)_3$ or $La(hfac)_3$ as shown in Figure 8.

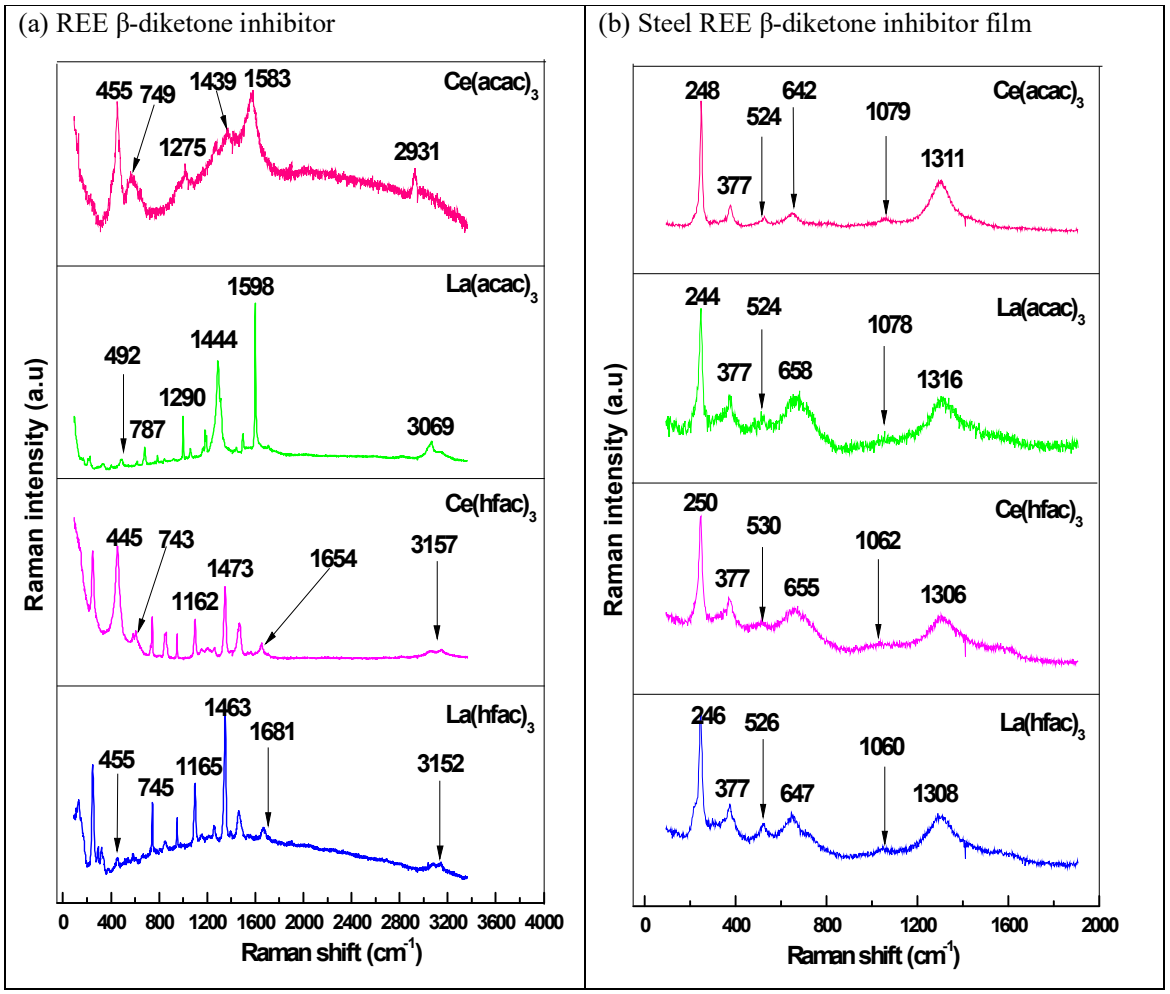

Figure 8: Raman spectra of $Ce(acac)_3$, $La(acac)_3$, $Ce(hfac)_3$and $La(hfac)_3$ inhibitors and the corrosion products formed on 304 and 316 SS.

Table 4: Raman frequency $Ce(acac)_3$, $La(acac)_3$, $Ce(hfac)_3$ and $La(hfac)_3$ inhibitors and the corrosion products formed on 304 and 316 SS.

Inhibitor $Ce(acac)_3$		Corrosion Product on 304 SS	
Frequency (cm^{-1})	Assignment	Frequency (cm^{-1})	Assignment
1583	C=O	248, 1311	α-Fe_2O_3
455	M-O	524	REE-O
2931	O-H	377	γ-FeOOH
Inhibitor $La(acac)_3$		Corrosion Product on 304 SS	
Frequency (cm^{-1})	Assignment	Frequency (cm^{-1})	Assignment
1598	C=O	244, 1306	α-Fe_2O_3
492	M-O	524	REE-O
3069	O-H	377	γ-FeOOH
Inhibitor $Ce(hfac)_3$		Corrosion Product on 316 SS	
Frequency (cm^{-1})	Assignment	Frequency (cm^{-1})	Assignment
1654	C=O	250, 1306	α-Fe_2O_3
445	M-O	530	REE-O
3157	O-H	377	γ-FeOOH
Inhibitor $La(hfac)_3$		Corrosion Product on 316 SS	
Frequency (cm^{-1})	Assignment	Frequency (cm^{-1})	Assignment
1681	C=O	246, 1308	α-Fe_2O_3
455	M-O	526	REE-O
3152	O-H	377	γ-FeOOH

4.3 Fourier Transform Infrared Spectroscopy (Ftir)

Fourier Transform Infrared spectroscopy (FTIR) was used to characterise further the REE β-diketone inhibitors and the films that were formed on the surface of the two stainless steel samples (304 & 316) after electrochemical corrosion tests in the solutions containing a 0.5% concentration of the REE β-diketone inhibitor (Figure 9). The bands associated with the functional groups of the synthesised REE β-diketone complexes were all assigned according to that in the literature [21,32]. The appearance of a band in the region 583 and 518 cm^{-1} indicates the bonding of the metal ion with the β-diketone molecules and can be ascribed to the M-O vibration [20,21,33–35]. The main functional groups present in REE β-diketone that are responsible for film formation on the steel, are the carbonyl functional group and enolic structure. It was observed that the frequency band of the enolic structure and the carbonyl functional group that appear on the metal surface shifted to a lower frequency compared to the frequencies noted for the synthesised REE β-diketone complexes.

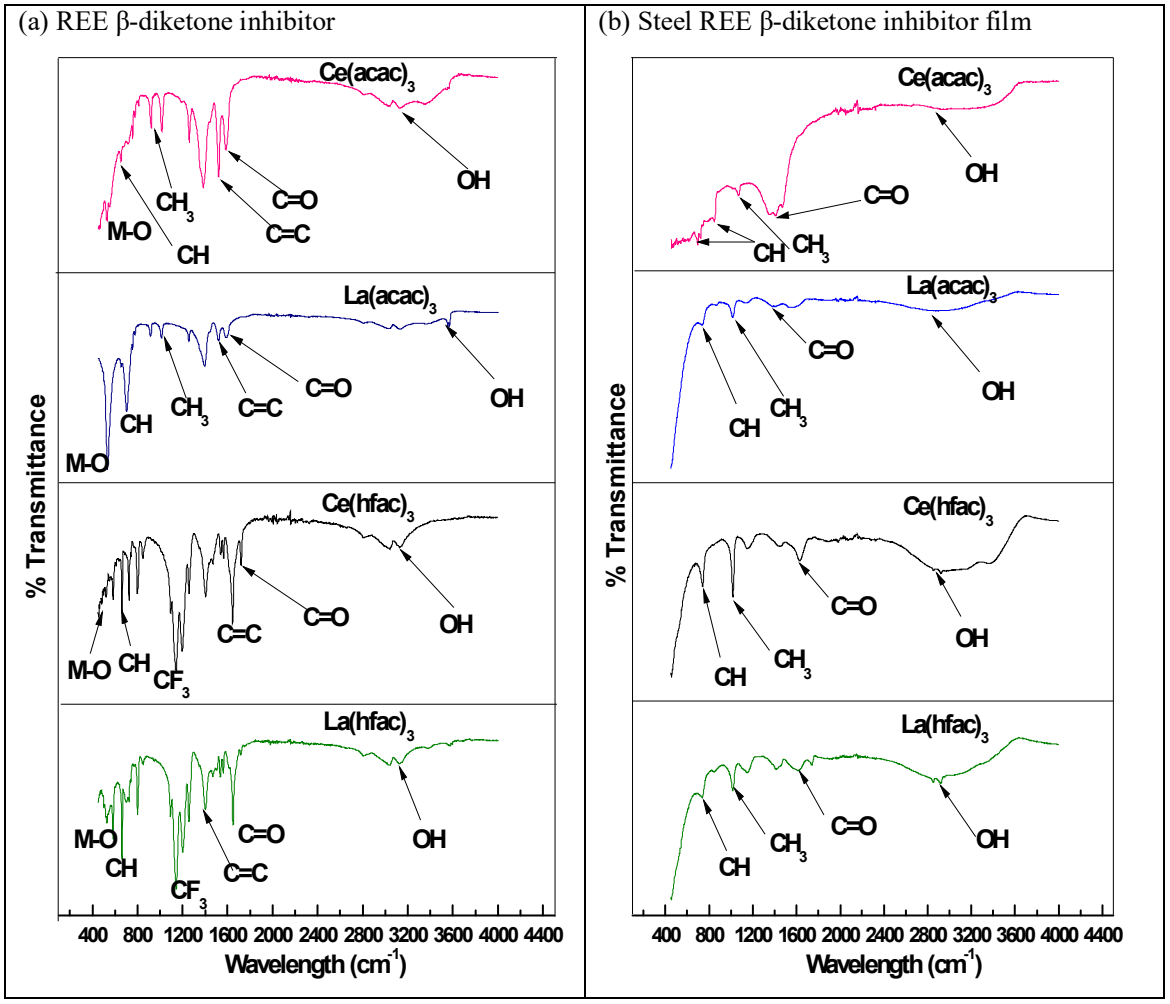

Figure 9: IR spectra of $Ce(acac)_3$, $La(acac)_3$, $Ce(hfac)_3$and $La(hfac)_3$ inhibitors and the corrosion products formed on 304 and 316 SS.

V. CONCLUSIONS

The SEM results proved that $Ce(acac)_3$, $La(acac)_3$, $Ce(hfac)_3$ and $La(hfac)_3$ efficiently inhibit the corrosion of 304 and 316 SS even at low concentration (0.5 % m/v) in 0.1 M HCl solution in the temperature range of 20-60°C. Raman spectroscopy confirmed that the complexes form a rare earth oxide/hydroxide containing film on the surface of the samples. Iron oxide/hydroxide on the surface of the steels were also observed. According to the potentiodynamic polarisation results, $Ce(acac)_3$, $La(acac)_3$, $Ce(hfac)_3$ and $La(hfac)_3$ act as cathodic inhibitors in HCl solution which led to a shift in the corrosion potential in a negative direction. The slight decreases in the Tafel slope values when the two inhibitors were added compared to the cases when no inhibitors were present, is further confirmation that all the tested REE β-diketone compounds act as cathodic inhibitors. All the inhibitors had a nearly similar inhibition efficiency as calculated from the potentiodynamic polarisation data. This corresponds to the observations made with the mass loss test results.

Funding: This research received no external funding.

Conflict Of Interest: The authors declare no financial or commercial conflict of interest.

Data Availability Statement: The data that support the findings contained within the article.

Author Contributions: Olatunde .J. Lawal performed the experiments, data analysis and writing-original draft. Johannes .H. Potgieter was

involved in conceptualisation, supervision, project management, writing-review and editing.

REFERENCES

1. Nandurkar, N.S.; Patil, D.S.; Bhanage, B.M. Ultrasound assisted synthesis of metal-1,3-diketonates. *Inorg. Chem. Commun.* 2008, *11*, 733–736, doi:10.1016/ j.inoche. 2008.03.014.
2. Verma, P.N.; Sheikh, J.I.; Juneja, H.D. Synthesis of β-diketone and its Metal Complexes. *World Appl. Sci. J.* 2011, *14*, 1154–1157.
3. Bhise, N.A., Ashwini A. Agale, A.A., Gaikwad S.T.; Rajbhoj, A.S. Synthesis and Characterization of Mn(II), Fe(III), Co(II), Ni(II) and Cu(II) Complexes of β-Diketone. *Asian J. Chemistry* 2017, *29*, 2372–2378.
4. Amadeh, A.; Allahkaram, S.R.; Hosseini, S.R.; Moradi, H.; Abdolhosseini, A. The use of rare earth cations as corrosion inhibitors for carbon steel in aerated NaCl solution. *Anti-Corrosion Methods Mater.* 2008, *55*, 135–143, doi:10.1108/00035590810870446.
5. Matter, E.A.; Kozhukharov, S.; Machkova, M.; Kozhukharov, V. Comparison between the inhibition efficiencies of Ce(III) and Ce(IV) ammonium nitrates against corrosion of AA2024 aluminum alloy in solutions of low chloride concentration. *Corros. Sci.* 2012, *62*, 22–33, doi:10.1016/j.corsci.2012.03.039.
6. Fouda, A.S.; Abd El-Wahab, S.M.; Attia, M.S.; Youssef, A.O.; Elmoher, H.O. Rare earth metals as eco-friendly corrosion inhibitors for mild steel in produced water. *Der Pharma Chem.* 2015, *7*, 74–87.
7. Boudellioua, H.; Hamlaoui, Y.; Tifouti, L.; Pedraza, F. Effects of polyethylene glycol (PEG) on the corrosion inhibition of mild steel by cerium nitrate in chloride solution. *Appl. Surf. Sci.* 2019, *473*, 449–460, doi:10.1016/ j.apsusc.2018.12.164.
8. Boudellioua, H.; Hamlaoui, Y.; Tifouti, L.; Pedraza, F. Effect of the temperature of cerium nitrate–NaCl solution on corrosion inhibition of mild steel. *Mater. Corros.* 2020, *71*, 1300–1309, doi:10.1002/maco.201911472.
9. Dastgheib, A.; Mohammadzadeh Attar, M.; Zarebidaki, A. Evaluation of Corrosion Inhibition of Mild Steel in 3.5 wt% NaCl Solution by Cerium Nitrate. *Met. Mater. Int.* 2020, *26*, 1634–1642, doi:10.1007/s12540-019-00432-x.
10. Ait Albrimi, Y.; Ait Addi, A.; Douch, J.; Souto, R.M.; Hamdani, M. Inhibition of the pitting corrosion of 304 stainless steel in 0.5M hydrochloric acid solution by heptamolybdate ions. *Corros. Sci.* 2015, *90*, 522–528, doi:10.1016/j.corsci.2014.10.023.
11. Eguchi, K.; Ishiguro, Y.; Ota, H. Corrosion behavior of multi-phase stainless steel in 15% hydrochloric acid at a temperature of 80C. *Corrosion* 2015, *71*, 1398–1405, doi:10.5006/1754.
12. Zou, G.; Shi, W.; Xiang, S.; Ji, X.; Ma, G.; Ballinger, R.G. Corrosion behavior of 904L austenitic stainless steel in hydrofluoric acid. *RSC Adv.* 2018, *8*, 2811–2817, doi:10.1039/c7ra12453h.
13. Loto, R.T. Effect of elevated temperature variations on the corrosion resistance of S31603 and SS2562 austenitic stainless steels in chloride-sulphate environments. *J. Mater. Res. Technol.* 2019, *8*, 5415–5421, doi:10.1016 / j.jmrt.2019.09.008.
14. Woldemedhin, M.T.; Srinivasan, J.; Kelly, R.G. Effects of environmental factors on key kinetic parameters relevant to pitting corro sion. *J. Solid State Electrochem.* 2015, *19*, 3449–3461, doi:10.1007/s10008-015- 2816-9.
15. Shakir, I.K.; Mohammed, A.-K. M. A; Alsamurraee, A.; Mahdi, Saleh, S. M. Pitting Corrosion Behavior of 304 SS and 316 SS Alloys in Aqueous Chloride and Bromide Solutions. *J. Eng.* 2018, *24*.
16. Ghanbari, M. M. Attar, M.M. AceA. Ghanbari, M. M. Attar, M. M. (2009). Acetylacetonate Complexes as New Corrosion Inhibitors in Phosphoric Acid Media. Progress in Color, Colorants and Coating, 2, 115–122. *Prog. Color. Color. Coat.* 2009, *2*, 115–122.
17. Somers, A.E.; Hinton, B.R.W.; Bruin -dickason, C. De; Deacon, G.B.; Junk, P.C.; Forsyth, M. New , environmentally friendly , rare earth carboxylate corrosion inhibitors for mild steel. *Corros. Sci.* 2018, *139*, 430–437, doi:10.1016/j.corsci.2018.05. 17.
18. Markley, T.A.; Forsyth, M.; Hughes, A.E. Corrosion protection of AA2024-T3 using rare

earth diphenyl phosphates. *Electrochim. Acta* 2007, *52*, 4024–4031, doi:10.1016/ j.electacta. 2006.11.028.
19. Krishnankutty, K.; Ummathur, M.B.;Ukken, M.P. Some unsaturated β-diketones and their metal chelates. *Analytical Chemistry* 2009, *6*, 4–8.
20. Ukken, M.P.; Ummathur, M.B. Synthesis and characterization of two conjugated β-diketones and their metal complexes. *Arch. Appl. Sci. Res.* 2013, *5*, 247–250.
21. Nath, P.; Bharty, M.K.; Dani, R.K.; Tomar, M.S.; Acharya, A. Mn(II), Co(III), Ni(II), Cd(II) and Cu(II) Complexes of 2-The noyltrifluoroacetone: Syntheses, Structures, Photoluminescence, Thermal, Electrochemical and Antitumor Studies on Dalton's Lymphoma Cells. *ChemistrySelect* 2017, *2*,10449–10458, doi:10.1002/slct.20170 2036.
22. Andersen, A.B.A.; Pyykkönen, A.; Jensen, H.J.A.; McKee, V.; Vaara, J.; Nielsen, U.G. Remarkable reversal of 13C-NMR assignment in d1, d2 compared to d8, d9 acetylacetonate complexes: Analysis and explanation based on solid-state MAS NMR and computations. *Phys. Chem. Chem. Phys.* 2020, *22*, 8048–8059, doi:10.1039/d0cp00980f.
23. Desa, M.N.; Desai, M.B. Carbonyl compounds as corrosion inhibitors for mild steel in HCl solutions. *Corros. Sci.* 1984, *24*, 649–660.
24. Peng, Y.; Hughes, A.E.; Deacon, G.B.; Junk, P.C.; Hinton, B.R.W.; Forsyth, M.; Mardel, J.I.; Somers, A.E. A study of rare-earth 3-(4-methylbenzoyl)-propanoate compounds as corrosion inhibitors for AS1020 mild steel in NaCl solutions. *Corros. Sci.* 2018, *145*, 199–211, doi:10.1016/j.corsci.2018.09.022.
25. Nam, N.D.; Thang, V.Q.; Hoai, N.T.; Hien, P. V. Yttrium 3-(4-nitrophenyl)-2-propenoate used as inhibitor against copper alloy corr osion in 0.1 M NaCl solution. *Corros. Sci.* 2016, *112*, 451–461, doi:10.1016/j.corsci. 2016. 08.005.
26. Tsaryuk, V.I.; Zhuravlev, K.P.; Szostak, R.; Vologzhanina, A. V. Structure, Luminescence, and Raman Spectroscopy of europium and terbium dipivaloylmethanates and other β-diketonates with 2,2′-bipyridine. *J. Struct. Chem.* 2020, *61*, 1026–1037, doi:10.1134/ S0022476620070045.
27. Boudellioua, H.; Hamlaoui, Y.; Tifouti, L.; Pedraza, F. Comparison Between the Inhibition Efficiencies of Two Modification Processes with PEG–Ceria Based Layers Against Corrosion of Mild Steel in Chloride and Sulfate Media. *J. Mater. Eng. Perform.* 2017, *26*, 4402–4414, doi:10.1007/ s11665-017-2867-4.
28. De Faria, D.L.A.; Venâncio Silva, S.; De Oliveira, M.T. Raman microspectroscopy of some iron oxides and oxyhydroxides. *J. Raman Spectrosc.* 1997, *28*, 873–878, doi:10.1002/(sici)10974555(199711)28:11<873 ::aid-jrs177>3.0.co;2-b.
29. Jubb, A.M.; Allen, H.C. Vibrational spectroscopic characterization of hematite, maghemite, and magnetite thin films produced by vapor deposition. *ACS Appl. Mater. Interfaces* 2010, *2*, 2804–2812, doi:10.1021/am1004943.
30. Święch, D.; Paluszkiewicz, C.; Piergies, N.; Pieta, E.; Lelek-Borkowska, U.; Kwiatek, W. Identification of corrosion products on Fe and Cu metals using spectroscopic methods. *Acta Phys. Pol. A* 2018, *133*, 286–288, doi:10.12693/APhysPolA.133.286.
31. Criado, M.; Martínez-Ramirez, S.; Bastidas, J.M. A Raman spectroscopy study of steel corrosion products in activated fly ash mortar containing chlorides. *Constr. Build. Mater.* 2015, *96*, 383–390, doi:10.1016/j.conbuild mat.2015.08.034.
32. Song, H.; Jiang, Y.; Xia, C.; Meng, G.; Peng, D. Synthesis and characterization of volatile metal β-diketonate chelates of M (DPM) n (M = Ce, Gd, Y, Zr, n = 3, 4) used as precursors for MOCVD. *Journal of Crystal Growth*. 2003, *250*, 423–430, doi:10.1016/ S0022-0248(02)02413-2.
33. Al-Wassil, A.I.; Al-Farhan, K.A.; Mukhalalati, M.; Mahfouz, R.M. Coordination Chemistry of Thenoyltrifluoroacetone 1- synthesis and Characterization of In3+- the noyltrifluoro-acetone Complex. *Spectrosc. Lett.* 1998, *31*, 299–305, doi:10.1080/00387019 808003254.
34. Kumar, M.; Sharma, T.R. Synthesis, characterization and properties of metal